Surface fitting in SPECT imaging useful for Detecting Parkinson's Disease and Scans Without Evidence of Dopaminergic Deficit

R. Prashanth*, Sumantra Dutta Roy
Department of Electrical Engineering, Indian Institute of technology Delhi, New Delhi 110016, India
(*Corresponding author) RP email: eez108051@ee.iitd.ac.in, SDR email: sumantra@ee.iitd.ac.in

Pravat K. Mandal
Neurospectroscopy and Neuroimaging Laboratory, National Brain Research Centre, 122050, India
email: pravat@nbrc.ac.in

Shantanu Ghosh
Martinos Center for Biomedical Imaging, Massachusetts General Hospital and Harvard Medical School, Boston, Massachusetts, USA
email:shantanu@nmr.mgh.harvard.edu

***Abstract*— Dopaminergic imaging using Single Photon Emission Computed Tomography (SPECT) with ^{123}I-Ioflupane have shown to increase the diagnostic accuracy in Parkinson's Disease (PD). Studies show that around 10% of subjects who are clinically diagnosed as PD, have SPECT scans in the normal range and are called Scans Without Evidence of Dopaminergic Deficit (SWEDD) subjects. Subsequent follow-up on these subjects has indicated that they are unlikely to have PD. Detection and differentiation of PD and SWEDD is problematic in the early stages of the disease. Early and accurate diagnosis of PD and also SWEDD is crucial for early management, avoidance of unnecessary medical examinations and therapies; and their side-effects. We in our paper, use the SPECT images from 35 Normal, 36 PD and 38 SWEDD subjects as obtained from the Parkinson's Progression Markers Initiative (PPMI) database, to carry out intensity-based surface fitting using polynomial model. This is the first time that such kind of modeling is carried out on the SPECT images for the characterization of PD. Our results show that the surface profile in terms of model coefficients and goodness-of-fit parameters is different for Normal, Early PD and SWEDD subjects. Such kind of modeling may aid in the diagnosis of early PD and SWEDD from SPECT images.**

Keywords*— *Parkinson's disease, Early diagnosis, SPECT imaging, Image Segmentation, Surface fitting, Polynomial models

I. INTRODUCTION

Early and accurate diagnosis of PD and SWEDD is crucial for several reasons: early management, avoidance of unnecessary medical examinations and therapies; and their associated financial costs, side-effects and safety risks [1, 2]. However, the Parkinson's Progression Markers Initiative (PPMI) [3], which is the first large-scale study to explore and identify PD progression markers, points out that early diagnosis of *de novo* PD subjects, like those being recruited for PPMI, is difficult because the cardinal symptoms and signs are mild or subtle (PPMI Study Protocol, http://www.ppmi-info.org/wp-content/uploads/2011/11/PPMI-Protocol-Amd3.pdf).

Single Photon Emission Computed Tomography (SPECT) with ^{123}I-Ioflupane (DaTSCAN^{TM}, GE Healthcare; also known as [^{123}I]FP-CIT) is most useful, at least in cases when there is diagnostic uncertainty especially during the early stage of the disease. An abnormal SPECT scan (showing dopamine transporter concentration deficit) strongly supports the diagnosis of neurodegenerative parkinsonism, due to which SPECT scanning increases the accuracy of diagnosis and thereby are increasingly becoming valuable tool for the clinician [2]. Studies show that around 10% of subjects, who are clinically diagnosed as Parkinson's Disease (PD), have SPECT scans in the normal range and are called as Scans Without Evidence of Dopaminergic Deficit (SWEDD) subjects [1]. Subsequent follow-up on these subjects have indicated that they are unlikely of having PD [4, 5].

Intensity distribution in the SPECT image at the striatum (which is composed of caudate nucleus and putamen) is an important feature that distinguishes normal from abnormal scans [6]. A normal scan (Fig. 2(a)) is one in which there is distinct and bilateral striatal activity and is seen as two comma or crescent-shaped focal regions of activity, on each side of the hemisphere, that are largely symmetric; and anything other than this structure is an abnormal scan. In PD, the comma shaped regions of activity gets changed to roughly circular or oval foci structures on one or both sides of the hemisphere (Fig. 2(b)) [6].

Surface fitting is a popular technique and has been used in many applications in biomedicine, like in the detection of corneal anterior surface [7], skull's surface fitting [8], lung lobe identification [9] and colonic polyp detection [10]. Surface fitting using implicit polynomial functions in x, y, z of degree greater than 2 are useful in representing surfaces that are more complicated than that can be represented by quadric surfaces (e.g., ellipsoid, paraboloid, etc.) [11-13]. Our basic idea in the paper is that to fit a 3-D polynomial model (surface) based on the intensities, from the high intensity regions that are or part of the striatum, from SPECT imaging and to understand how these surfaces (or intensity distributions) change in Normal, SWEDD and Early PD subjects which thereby, may aid in the early diagnosis of PD. As per our knowledge, this is the first time that such kind of study using surface fitting is used for the characterization of PD. We perform surface fitting using a third-degree (cubic) polynomial model, based on the intensity in the SPECT images of Normal, Early PD and SWEDD subjects.

II. MATERIALS AND METHODS

The flowchart of the analysis carried out in the paper is as shown in Fig. 1.

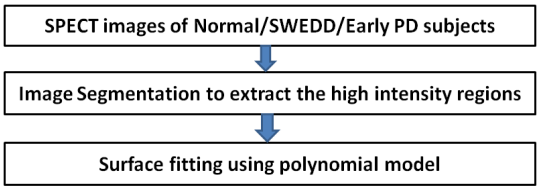

Fig. 1. Flow chart of the analysis carried out

A. Database

For our experiments, we used the data obtained from the Parkinson's Progression Markers Initiative (PPMI) database (www.ppmi-info.org/data). For up-to-date information on the study, visit www.ppmi-info.org. The PPMI [3] is a comprehensive, observational, international, multi-center, longitudinal and the first large-scale study, that mainly recruits early and untreated PD subjects, to identify PD progression biomarkers. For our experiments, we use SPECT images from 35 Normal, 36 Early PD (mean Hoehn and Yahr (HY) Stage of 1.86) and 38 SWEDD (mean HY stage of 1.33) subjects that are obtained from the PPMI database.

B. Image Segmentation

Image segmentation was carried out to segment out the high intensity regions that are part of the striatum. The PPMI Central SPECT Core Lab, which performed the reconstruction of the image from raw projection data, including attenuation correction based on phantoms acquired on the day the subject was imaged, also performed the spatial normalization of images to create consistent orientation (PPMI Imaging Core Update, http://www.ppmi-info.org/wp-content/uploads/2012/05/03_-PPMI_02_May_2012-Annual-mtg_Imaging_JS.pdf). Among the 91 slices in each 3D SPECT scan, the 42nd slice (2D image) was chosen for further analysis as it clearly showed the high activity region corresponding to the striata. The image segmentation is carried out in 2 steps as explained below.

1) Preprocessing

Preprocessing of the images was necessary to make a consistent intensity range for each input image. This was carried out by image normalization in which each image is converted in the range [0,1] using

$$I_{new} = \frac{I - I_{min}}{I_{max} - I_{min}} \quad (1)$$

where I_{new} is the normalized intensity, I is the input value of intensity, I_{min} is the minimum intensity, I_{max} is the maximum intensity.

2) Binarization and image segmentation

Followed by preprocessing, image segmentation was carried out, to extract the high intensity regions that corresponded to the striata. A threshold was selected such that it best segmented the high intensity region. This image binarization produces a mask image which is then, used to segment the true region from the original unprocessed image.

C. Surface fitting using Polynomial model

For our experiments, we have used third-degree (cubic) polynomial for fitting and it is given by

$$z(x,y) = p_{00} + p_{10} * x + p_{01} * y + p_{20} * x^2 + p_{11} * x * y + p_{02} * y^2 + p_{30} * x^3 + p_{12} * x * y^2 + p_{21} * x^2 * y + p_{03} * y^3 \quad (2)$$

where the model coefficients p_{ij} ; $i,j = 0,1,2,3$; are estimated by linear least-squares method that minimizes the summed square of residuals (or errors) (SE) which is given by

$$SE = \sum_{i=1}^{n} r_i^2 = \sum_{i=1}^{n} \left(z_i(x,y) - \hat{z_i}(x,y) \right)^2 \quad (3)$$

where n is number of data points and r_i is the residual for the i^{th} data point, $z_i(x,y)$ is the observed response value and $\hat{z_i}(x,y)$ is the fitted response value. Data was normalized by centering it at zero mean and scaling it to unit standard deviation to remove any scaling problems.

1) Evaluating the goodness of fit

(i) The sum of squares due to error (SE)

It measures the total deviation of the response values from the fit and is given by Eqn. (3). A value closer to 0 indicates the fit is good and is useful for prediction.

(ii) R^2

R^2 indicates the goodness of fit in explaining the variation in the data. It is measured as the square of the correlation between the response values and the predicted response values and is given by

$$R^2 = 1 - \frac{SE}{SM} \quad (4)$$

where SM is the sum of squares about the mean and is given by $SM = \sum_{i=1}^{n} \left(z_i(x,y) - \overline{z(x,y)} \right)^2$ where $\overline{z(x,y)}$ is the mean of observed response value $z_i(x,y)$.

An R^2 value closer to 1 shows a better fit indicating that the model accounts for a greater proportion of variance.

(iii) Adjusted R^2 (R^2_{adj})

When the number of fitted coefficients in the model increases, R^2 will increase although the fit may not improve in a practical sense. To avoid this situation, adjusted R^2 can be used which adjusts R^2 based on the residual degrees of freedom (which depends on the number of fitted coefficients). The residual degrees of freedom (dfe) is given by

$$dfe = n - k \quad (5)$$

where n is the number of response values and k is the number of fitted coefficients

The Adjusted R^2 (R^2_{adj}) is given by

$$R^2_{adj} = 1 - \frac{SE * (n-1)}{SM * (dfe)} = 1 - \left[\frac{(1-R^2)(n-1)}{n-k}\right] \quad (6)$$

R^2_{adj} can taken values from 0 to 1 and value closer to 1 indicate a better fit.

(iv) Root mean squared error (RMSE)

It is an estimate of the standard deviation of the random component in the data and is given by

$$RMSE = \sqrt{\frac{SE}{dfe}} = \sqrt{\frac{SE}{n-k}} \quad (7)$$

III. Results and Discussion

Fig. 2 shows the input image, image after segmentation of high intensity region, and the 3-D plot of points and the fitted polynomial surface for Normal (a, b, c), Early PD (d, e, f), and SWEDD (g, h, i) subject.

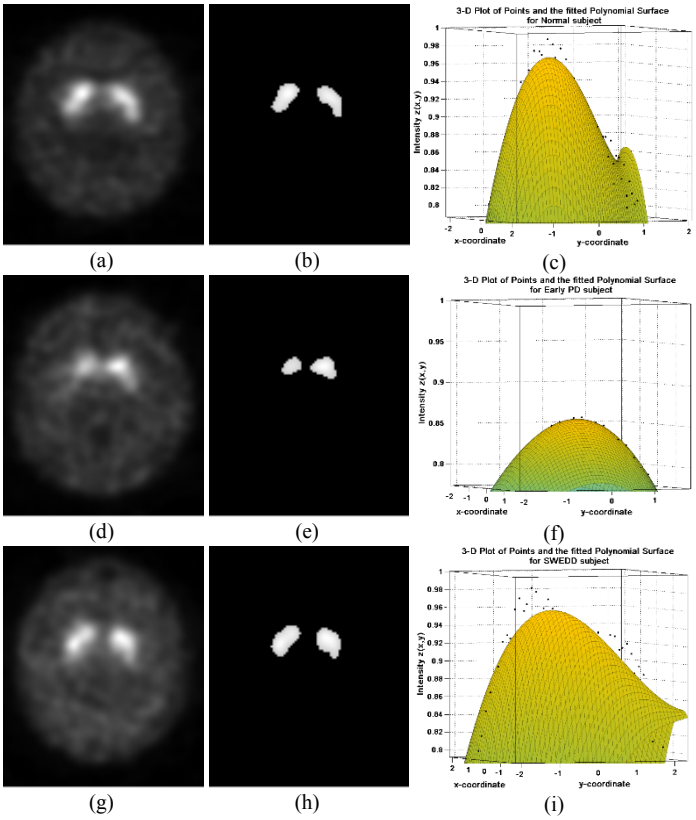

Fig. 2. (a, b, c) are the input image, image after segmentation of high intensity regions, and the 3-D plot of points and fitted polynomial surface, respectively, for a Normal subject. Similarly, (d, e, f) are images for Early PD subject and (g, h, i) are images for SWEDD subject.

Fig. 3. shows the box plots of the values of the model coefficients and the goodness of fit measures for Normal, Early PD and SWEDD. Table I shows the mean values of the model coefficients and the goodness of fit measures for Normal, Early PD and SWEDD. It is observed that, in the case of Early PD, all the model coefficients and goodness of fit measures show good amount of variation as compared to Normal or SWEDD subjects. This is because the shape of the polynomial model changes during PD which is due to the change of comma shaped region as in normal, to circular dot or oval shaped region in PD. The goodness of fit measures R^2 and R^2_{adj} increases in PD indicating that the fit is becoming more accurate in PD. *dfe* which depends on the number of points in the segmented region decreases in PD because the high intensity region is reduced in PD. Comparing Normal and SWEDD, it is observed that the model coefficients are almost similar for Normal and SWEDD subjects. However, the goodness of fit measures of R^2, degrees of freedom (*dfe*) and adjusted R^2 (R^2_{adj}) show variation and they are slightly higher in the case of Normal indicating that there is higher amount of misfit in the case of SWEDD.

TABLE I
MEAN VALUES OF THE MODEL COEFFICIENTS AND GOODNESS OF FIT MEASURES FOR NORMAL, EARLY PD AND SWEDD

	p_{00}	p_{10}	p_{01}	p_{20}	p_{11}	p_{02}	p_{30}	p_{21}
Normal	0.941	-0.017	-0.038	-0.057	-0.065	-0.057	0.008	0.010
Early PD	0.909	0.005	-0.015	-0.034	-0.015	-0.034	0	0.005
SWEDD	0.939	-0.014	-0.038	-0.052	-0.062	-0.052	0.008	0.011

	p_{12}	p_{03}	*SE*	R^2	*dfe*	R^2_{adj}	*RMSE*
Normal	0.005	0.012	0.013	0.947	98.30	0.942	0.011
Early PD	-0.003	0.003	0.004	0.971	52.33	0.967	0.006
SWEDD	0.005	0.012	0.017	0.911	90.75	0.902	0.013

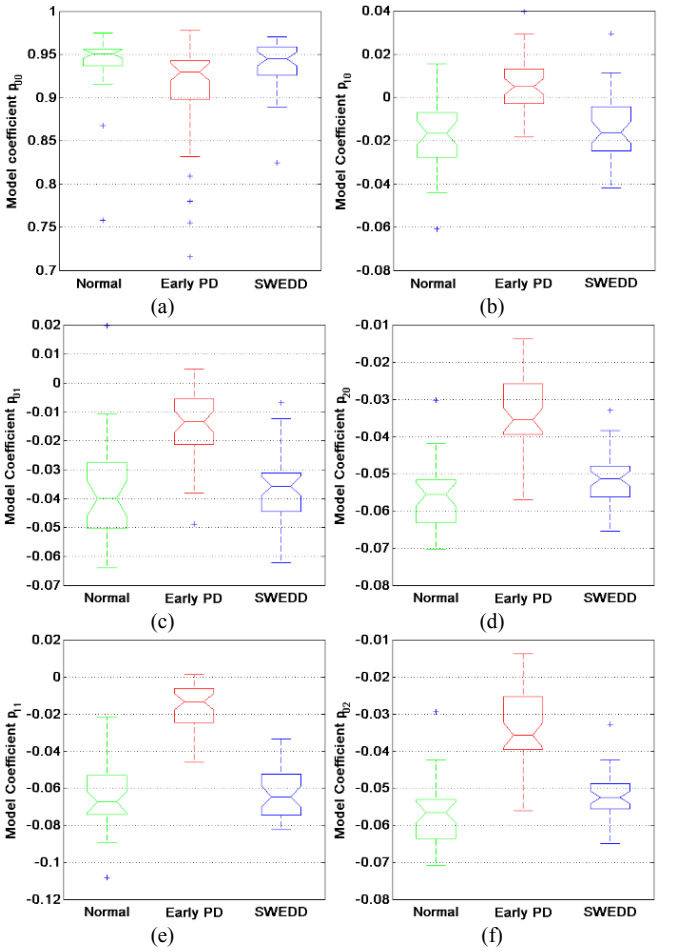

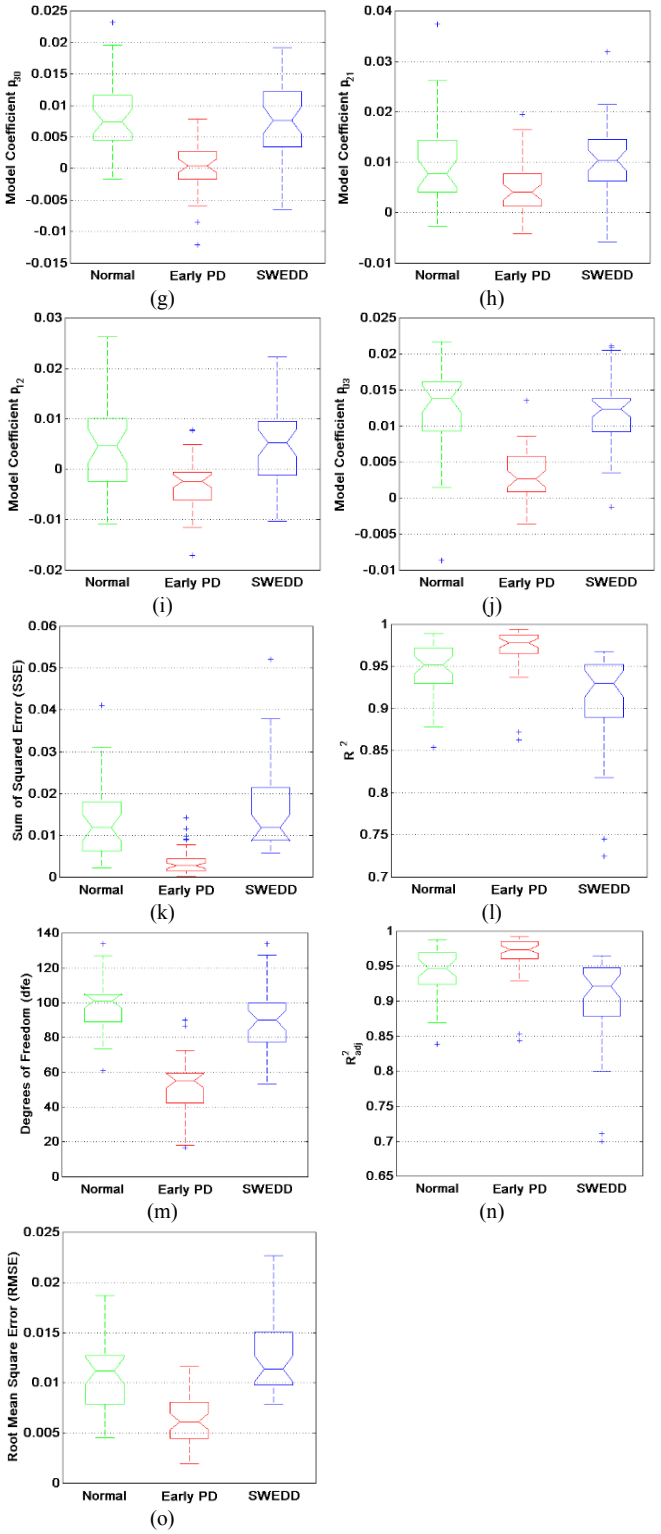

Fig. 3. Box plots of the model coefficients (a) p_{00}, (b) p_{10}, (c) p_{01}, (d) p_{20}, (e) p_{11}, (f) p_{02}, (g) p_{30}, (h) p_{21}, (i) p_{12}, (j) p_{03}; and goodness of fit measures (k) SE, (l) R2, (m) dfe, (n) R^2_{adj}, (o) RMSE for Normal, Early PD and SWEDD.

IV. CONCLUSION

Dopaminergic imaging using Single Photon Emission Computed Tomography (SPECT) with ^{123}I-Ioflupane have shown to increase the accuracy of diagnosis of PD, even in the early stages of the disease. Studies show that around 10% of clinically diagnosed PD subjects have normal SPECT scans when assessed visually. In this study, we performed surface fitting, based on the intensities from the high intensity regions from the striatal region, using polynomial models. We observed that there is good amount of variation in the model coefficients and goodness-of -fit parameters between Early PD and Normal or SWEDD subjects; and slight variation of goodness of fit measures for SWEDD as compared to Normal. Hence, it is inferred that such kind of modeling may aid in the diagnosis of early PD and SWEDD.

ACKNOWLEDGMENT

PPMI – a public-private partnership – is funded by the Michael J. Fox Foundation for Parkinson's Research and funding partners, including [list the full names of all of the PPMI funding partners found at www.ppmi-info.org/fundingpartners]. Authors also thank Prof. Santanu Chaudhury and Prof. Prem Kalra for their valuable comments.

REFERENCES

[1] P. Schwingenschuh, *et al.*, "Adult onset asymmetric upper limb tremor misdiagnosed as Parkinson's disease: A clinical and electrophysiological study," *Mov Disord,* vol. 25, pp. 560-9, Apr 15 2010.

[2] J. L. Cummings, *et al.*, "The role of dopaminergic imaging in patients with symptoms of dopaminergic system neurodegeneration," *Brain,* vol. 134, pp. 3146-66, Nov 2011.

[3] K. Marek, *et al.*, "The Parkinson Progression Marker Initiative (PPMI)," *Prog Neurobiol,* vol. 95, pp. 629-635, 2011.

[4] K. Marek, D. Jennings, and J. Seibyl, "Long-term follow-up of patients with scans without evidence of dopaminergic deficit (SWEDD) in the ELLDOPA study," *Neurology,* vol. 64 (Suppl. 1), p. A274, 2005.

[5] S. A. Schneider, *et al.*, "Patients with adult-onset dystonic tremor resembling parkinsonian tremor have scans without evidence of dopaminergic deficit (SWEDDs)," *Movement Disorders,* vol. 22, pp. 2210-5, Nov 15 2007.

[6] "DaTscan (Ioflupane I 123 injection) Prescribing Information," GE Healthcare2011.

[7] Z. Zhu, E. Janunts, T. Eppig, T. Sauer, and A. Langenbucher, "Iteratively re-weighted bi-cubic spline representation of corneal topography and its comparison to the standard methods," *Z Med Phys,* vol. 20, pp. 287-98, 2010.

[8] J. C. Carr, W. R. Fright, and R. K. Beatson, "Surface interpolation with radial basis functions for medical imaging," *IEEE Trans Med Imaging,* vol. 16, pp. 96-107, Feb 1997.

[9] J. Pu, *et al.*, "Pulmonary lobe segmentation in CT examinations using implicit surface fitting," *IEEE Trans Med Imaging,* vol. 28, pp. 1986-96, Dec 2009.

[10] A. Huang, R. M. Summers, and A. K. Hara, "Surface curvature estimation for automatic colonic polyp detection," presented at the Proc. SPIE 5746, Medical Imaging 2005: Physiology, Function, and Structure from Medical Images, 2005.

[11] D. Keren, D. Cooper, and S. Jayashree, "Describing Complicated Objects by Implicit Polynomials," *IEEE Trans. Pattern Anal. Mach. Intell.,* vol. 16, pp. 38-53, 1994.

[12] G. Taubin, "Estimation of Planar Curves, Surfaces, and Nonplanar Space Curves Defined by Implicit Equations with Applications to Edge and Range Image Segmentation," *IEEE Trans. Pattern Anal. Mach. Intell.,* vol. 13, pp. 1115-1138, 1991.

[13] J. Subrahmonia, D. B. Cooper, and D. Keren, "Practical Reliable Bayesian Recognition of 2D and 3D Objects Using Implicit Polynomials and Algebraic Invariants," *IEEE Trans. Pattern Anal. Mach. Intell.,* vol. 18, pp. 505-519, 1996.